Available online at www.sciencedirect.com
ScienceDirect
Trans. Nonferrous Met. Soc. China 25(2015) 22−29
Transactions of Nonferrous Metals Society of China
www.tnmsc.cn

Microstructures and mechanical properties of Mg−Al−Sm series heat-resistant magnesium alloys

Zheng-hua HUANG, Wen-jun QI, Jing XU, Chang CAI

Guangzhou Research Institute of Non-ferrous Metals, Guangzhou 510650, China

Received 8 January 2014; accepted 5 March 2014

Abstract: The microstructures and phase compositions of the as-cast and die-cast Mg−6.02Al−1.03Sm, Mg−6.05Al−0.98Sm−0.56Bi and Mg−5.95Al−1.01Sm−0.57Zn alloys were investigated. Meanwhile, the tensile mechanical and flow properties were tested. The results show that the as-cast microstructure of Mg−6.02Al−1.03Sm alloy is composed of α-Mg matrix, discontinuous β-$Mg_{17}Al_{12}$ phase and small block Al_2Sm phase with high thermal stability. Rod Mg_3Bi_2 phase precipitates when Bi is added, while the added metal Zn dissolves into α-Mg matrix and β-$Mg_{17}Al_{12}$ phase. The as-cast alloys exhibit the excellent tensile mechanical property. The tensile strength (σ_b) and elongation (δ) can reach 205−235 MPa and 8.5%−16.0% at ambient temperature, respectively. Meanwhile, they can also exceed 160 MPa and 14.0% at 423 K, respectively. The die-cast microstructures are refined obviously, and meanwhile the broken second phases distribute dispersedly. The die-cast alloys exhibit better tensile mechanical properties with the values of σ_b and δ of 240−285 MPa and 8.5%−16.5% at ambient temperature, respectively, and excellent flow property with the flow length of 1870−2420 mm. The die-cast tensile fractures at ambient temperature exhibit a typical character of ductile fracture.

Key words: heat-resistant magnesium alloy; Mg−Al−Sm alloy; microstructure; mechanical property; flow property; fracture morphology

1 Introduction

Magnesium alloys, one of the most important structural materials with high specific strength, are used widely in the automotive, communicated, electronic and aerial industries [1]. Mg−Al series alloys such as AZ91D and AM60B are the most widely used commercial heat-resistant magnesium alloys. However, the main strengthening phase β-$Mg_{17}Al_{12}$ exhibits low thermal stability owing to the low melting temperature of 710 K. When the temperature rises, the microstructure will become soft and coarse easily, and then the strength and creep resistance will decrease significantly. Thus, the alloys cannot usually be fabricated to the parts used under high temperature condition above 393 K for long time. Researchers often enhance the elevated temperature performance through precipitating the phases with high thermal stability such as Al_2Ca, Al_2Sr, Mg_2Si and Al−RE by adding alkaline earth metal [2−4], Si [5,6] and rare earth (RE) [7−13], respectively. RE with unique atomic electron and chemical property can purify the alloy melt, ameliorate the microstructure, and then enhance the mechanical property and corrosion resistance. Compared with other RE, the effects of cheaper Sm on the microstructure and mechanical properties of Mg−Al series alloys have been rarely studied yet [9,10]. Meanwhile, the addition of Bi can also enhance the elevated temperature performance effectively through precipitating the Mg_3Bi_2 phase with high thermal stability. Therefore, in this work, the microstructures, mechanical and flow properties of the as-cast and die-cast Mg−6.02Al−1.03Sm, Mg−6.05Al−0.98Sm−0.56Bi and Mg−5.95Al−1.01Sm−0.57Zn alloys were investigated, and the strengthening mechanism was discussed.

2 Experimental

The chemical compositions of the fabricated alloys were measured by inductively coupled plasma analyzer (ICP, JY Ultima2). The alloy ingots were prepared by melting Mg, Al, Bi, Zn and Mg−30%Sm (mass fraction) master alloy in an electric resistance furnace under the

Foundation item: Project (2013AA031001) supported by the National High-tech Research and Development Program of China; Project (2011A080403008) supported by the Major Science and Technology Project of Guangdong Province, China
Corresponding author: Zheng-hua HUANG; Tel/Fax: +86-20-37238039; E-mail: zhhuang@live.cn
DOI: 10.1016/S1003-6326(15)63574-9

mixed atmosphere of CO_2 and 0.1% SF_6 (volume fraction). When the melt temperature of Mg reached 1003 K, the pure metals and master alloy were added into the melt in turn. Then, the melt was stirred twice within 1 h to ensure the compositional homogeneity. After adding the refine agent, the melt was held at 1023 K for 25 min. When the temperature was cooled to 988 K, the melt was poured into the wedge permanent and spiral flow molds with the preheated temperature of 523 K, and then the samples for testing as-cast tensile and flow properties were obtained, respectively. The die-cast samples were obtained by a 400T die-casting machine with the injection force, injection time, cooling time and mold temperature of 370 kN, 4.0 s, 5 s and 463 K, respectively.

The specimens were etched with 4% HNO_3 (volume fraction) in ethanol. The microstructural observation was carried out on an optical microscope (OM, Leica DM IRM) and a scanning electron microscope (SEM, JEOL JXA−8100) with an energy dispersive spectroscope (EDS, OXFORD 7412). The phase analysis was carried out on an X-ray diffractometer (XRD, D/MAX-RC) with Cu K_α radiation. The tensile test at temperatures of 298 and 423 K was performed on a material test machine (GP−TS2000) at a rate of 2 mm/min. The tensile fractograph at ambient temperature was observed using SEM.

3 Results and discussion

3.1 Microstructure and mechanical property of as-cast alloys

Figure 1 shows the optical and SEM micrographs of the as-cast alloys. All as-cast microstructures consist

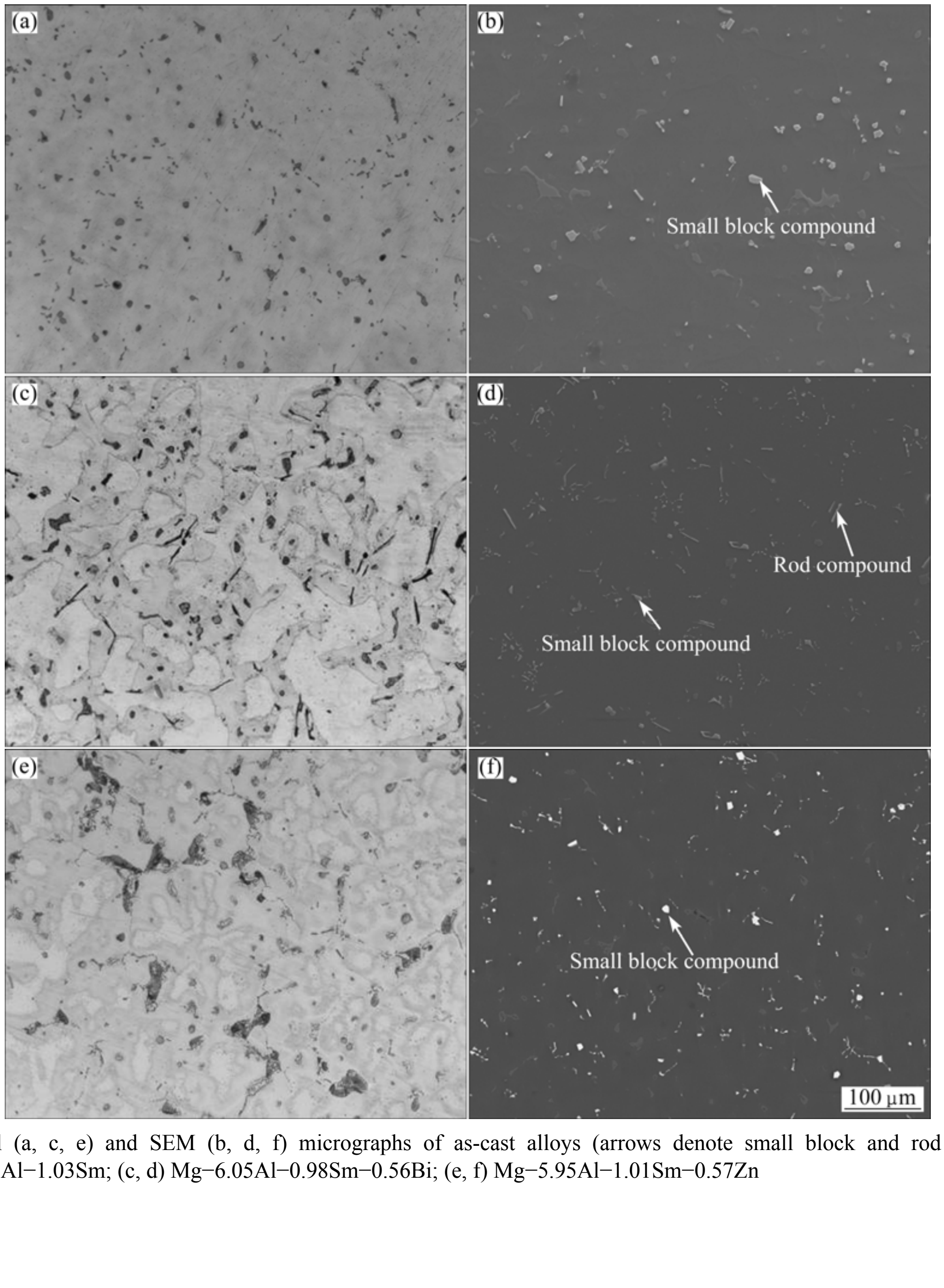

Fig. 1 Optical (a, c, e) and SEM (b, d, f) micrographs of as-cast alloys (arrows denote small block and rod compounds): (a, b) Mg−6.02Al−1.03Sm; (c, d) Mg−6.05Al−0.98Sm−0.56Bi; (e, f) Mg−5.95Al−1.01Sm−0.57Zn

of α-Mg matrix, few discontinuous β-$Mg_{17}Al_{12}$ phase and small block compound. In addition, rod compound can be observed in the microstructure of Mg−6.05Al−0.98Sm−0.56Bi alloy.

Figure 2 shows the EDS spectra of the as-cast alloys, and the results are listed in Table 1. It is seen that the gray phase is Mg−Al phase, i.e. β-$Mg_{17}Al_{12}$ for the three alloys. Small block compound is Al−Sm phase (spectrum 1 in Figs. 2(a) and (c) and spectrum 3 in Fig. 2(b). Rod compound is Mg−Bi phase containing few Al and Sm for Mg−6.05Al−0.98Sm−0.56Bi alloy (spectrum 1 in Fig. 2(b)). The added metal Zn dissolves into α-Mg matrix and β-$Mg_{17}Al_{12}$ phase.

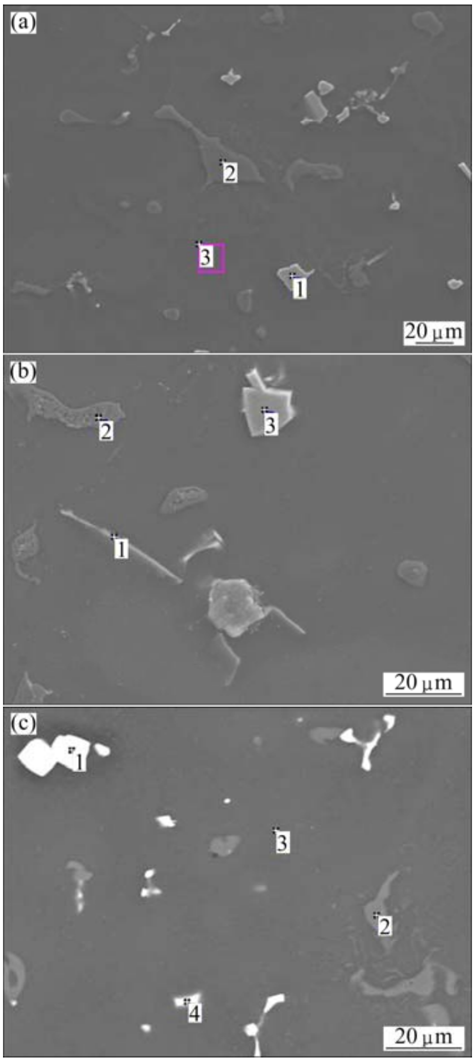

Fig. 2 EDS spectra of as-cast alloys: (a) Mg−6.02Al−1.03Sm; (b) Mg−6.05Al−0.98Sm−0.56Bi; (c) Mg−5.95Al−1.01Sm−0.57Zn

Figure 3 shows the XRD patterns of the as-cast alloys. It is seen that all XRD patters consist of peaks of α-Mg, β-$Mg_{17}Al_{12}$ and Al_2Sm phases. In addition, the peak of Mg_3Bi_2 phase can be observed among the XRD pattern of as-cast Mg−6.05Al−0.98Sm−0.56Bi alloy. Combined with the above mentioned EDS results, the small block and rod compounds are considered Al_2Sm and Mg_3Bi_2 phases, respectively.

Table 1 EDS results of as-cast alloys

Alloy	Position in Fig. 2	x(Mg)/%	x(Al)/%	x(Sm)/%	x(Bi)/%	x(Zn)/%
Mg−6.02Al−1.03Sm	1	0	64.52	35.48	0	0
	2	59.11	40.89	0	0	0
	3	99.82	0.18	0	0	0
Mg−6.05Al−0.98Sm−0.56Bi	1	75.12	4.95	5.53	14.40	0
	2	71.30	27.53	0	1.17	0
	3	0	67.07	32.93	0	0
Mg−5.95Al−1.01Sm−0.57Zn	1	0	66.69	33.31	0	
	2	65.11	30.06	0	0	4.83
	3	99.10	0	0	0	0.90
	4	37.59	44.51	17.90	0	0

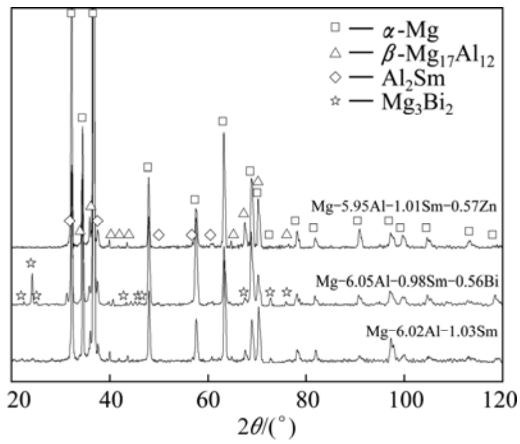

Fig. 3 XRD patterns of as-cast alloys

The degree of difficulty in forming compounds between different elements can be judged by electronegativity difference $\Delta\chi$. The greater the value of $\Delta\chi$ is, the larger the binding force is, and then the easier the formation of compounds is [14]. Electronegativities χ are 1.31, 1.61, 1.17 and 1.9 for elements Mg, Al, Sm and Bi, respectively [15]. Adding the RE into Mg−Al series alloys may form Al−RE, Mg−RE or Mg−Al−RE compounds. Sm−Al exhibits the larger value of $\Delta\chi$ (0.44) than Sm−Mg (0.14), which indicates the greater binding force between Sm and Al. From the thermodynamic point of view, small block Al_2Sm rather than Mg−Sm or Mg−Al−Sm phase precipitates on the priority when Sm is added into Mg−Al alloy. Meanwhile, Bi−Mg alloy exhibits larger value of $\Delta\chi$ (0.59) than Bi−Al alloy (0.29). Therefore, rod Mg_3Bi_2 compound can precipitate on the priority when Bi is added.

The as-cast alloys exhibit the excellent tensile mechanical property at ambient and elevated temperatures, respectively (Table 2). For Mg−6.02Al−1.03Sm alloy, tensile strength (σ_b) can reach 220 and 162 MPa at 298 and 423 K, respectively, and the corresponding elongation (δ) can reach 12.5% and 14.5%, respectively. At ambient temperature, σ_b and δ slightly decrease to 205 MPa and 8.5%, respectively when 0.56%Bi is added, while they slightly increase to 235 MPa and 16.0%, respectively when 0.57%Zn is added. Meanwhile, the two alloys exhibit the slightly higher comprehensive tensile mechanical property at elevated temperature.

Table 2 Tensile mechanical properties of as-cast and die-cast alloys

Alloy	Condition	σ_b/MPa		δ/%	
		298 K	423 K	298 K	423 K
Mg−6.02Al−1.03Sm	As-cast	220	162	12.5	14.5
	Die-cast	285	145	16.5	19.0
Mg−6.05Al−0.98Sm−0.56Bi	As-cast	205	162	8.5	19.5
	Die-cast	240	144	8.5	10.0
Mg−5.95Al−1.01Sm−0.57Zn	As-cast	235	171	16.0	20.0
	Die-cast	275	149	14.0	17.5

All as-cast tensile fractures at ambient temperature exhibit a complex mode of ductile and brittle fractures (Figs. 4(a), (c) and (e)). Dimples and cleavage steps exist simultaneously for Mg−6.02Al−1.03Sm alloy. Cleavage steps increase slightly when 0.56% Bi is added, which is consistent with the rapid decrease in the elongation. Dimples still increase slightly when 0.57% Zn is added, which is consistent with the slightly increasing comprehensive tensile mechanical property. Meanwhile, few fine second phase particles can be observed at the bottom of dimples for the three alloys (see illustrations).

The strengthening mechanism of magnesium alloys mainly includes the grain-refinement strengthening, solid−solution strengthening, precipitation strengthening, dispersion strengthening and strain hardening. During the

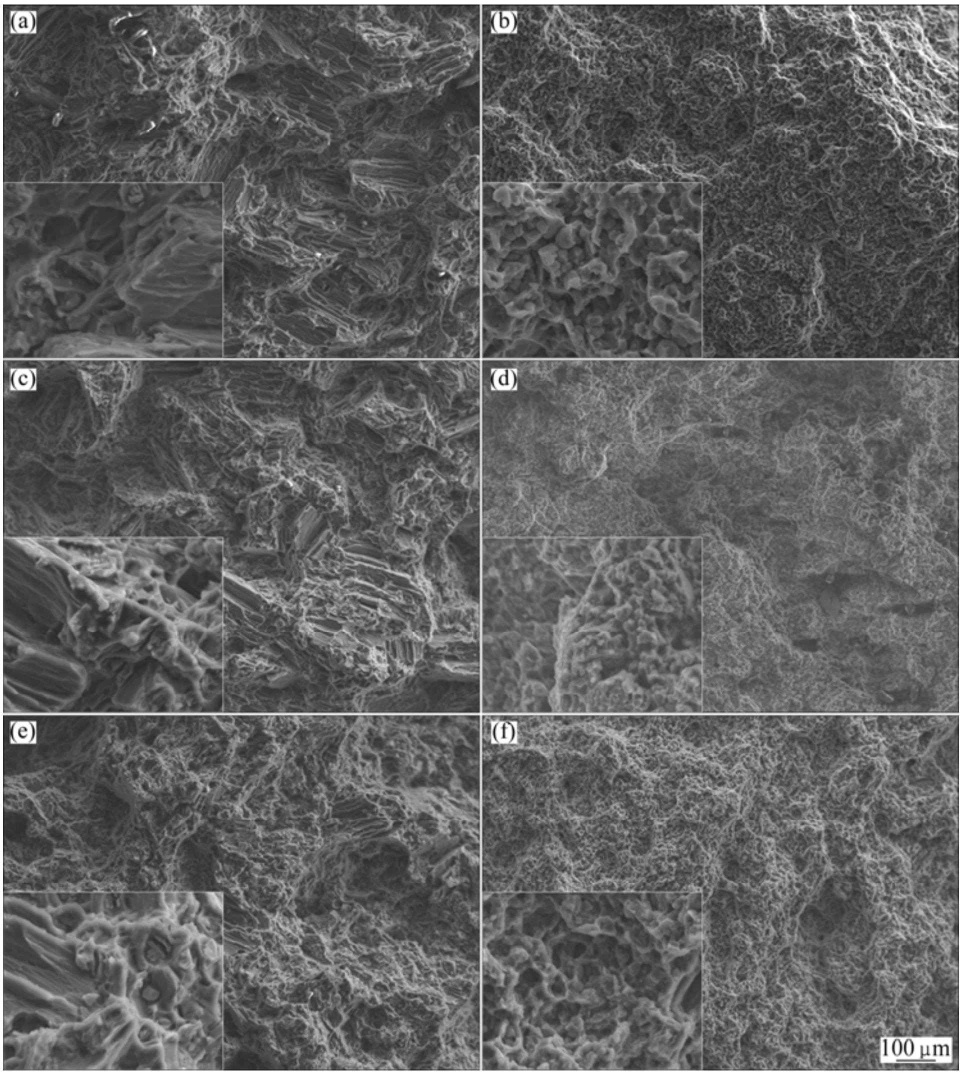

Fig. 4 SEM morphologies of tensile fractures of as-cast and die-cast alloys at ambient temperature (Illustrations indicate local enlarged regions): (a) Mg−6.02Al−1.03Sm, as−cast; (b) Mg−6.02Al−1.03Sm, die-cast; (c) Mg−6.05Al−0.98Sm−0.56Bi, as-cast; (d) Mg−6.05Al−0.98Sm−0.56Bi, die-cast; (e) Mg−5.95Al−1.01Sm−0.57Zn, as-cast; (f) Mg−5.95Al−1.01Sm−0.57Zn, die-cast

solidification process of Mg−6.02Al−1.03Sm alloy, Sm participates in the eutectic reaction to form small block Al_2Sm phase with high thermal stability, which can form the eutectic microstructure together with α-Mg and β-$Mg_{17}Al_{12}$ phases. Al_2Sm phase can be pushed into the growth interface, and then the free growth of dendrite can be impeded. Meanwhile, the second phases distribute dispersedly. The phase with high thermal stability can pin the grain boundary, and inhibit the sliding of the grain boundary and the movement of the dislocation at the elevated temperature effectively. Therefore, the as-cast alloy exhibits the excellent tensile mechanical property at ambient and elevated temperatures, respectively. When 0.56% Bi is added, the as-cast microstructure is not refined significantly. Meanwhile, new rod phase Mg_3Bi_2 plays a weaker strengthening effect than small block Al_2Sm phase. Therefore, the tensile mechanical property at ambient temperature decreases slightly. When 0.57% Zn is added, metal Zn dissolves into α-Mg matrix and β-$Mg_{17}Al_{12}$ phase, which leads to a slight increase in the tensile mechanical property at ambient and elevated temperatures owing to the solid−solution strengthening.

The as-cast alloys exhibit the relatively excellent flow property (Fig. 5(a)). The flow length can reach 460 mm for Mg−6.02Al−1.03Sm alloy. It decreases to 430 and 320 mm when 0.56% Bi and 0.57% Zn are added, respectively.

3.2 Microstructure and mechanical property of die-cast alloy

Figures 6 and 7 show the optical and SEM micrographs of the die-cast alloys, respectively. Obviously, the die-cast microstructures are different from those of the as-cast. The microstructures are refined significantly owing to the higher cooling rate. Meanwhile, the broken and refined second phases including discontinuous β-$Mg_{17}Al_{12}$, small block Al_2Sm and rod Mg_3Bi_2 phases mainly distribute along the grain boundary dispersedly.

The die-cast alloys exhibit better tensile mechanical properties at ambient temperature (Table 2). σ_b can increase to 285, 240 and 275 MPa for Mg−6.02Al−1.03Sm, Mg−6.05Al−0.98Sm−0.56Bi and Mg−5.95Al−1.01Sm−0.57Zn alloys with the increasing amplitude of 35−65 MPa, respectively. Meanwhile, the three alloys still exhibit the better plasticity, where δ is equal to or slightly higher than that of the as-cast value. This is owing to the grain-refining strengthening by the obviously refined microstructure and dispersion strengthening by the refined and dispersed second phases. Because gas cannot be exhausted opportunely and effectively during the commercial die-cast process, more or less gas cavities exist in the die-cast microstructures (see arrows in Fig. 7). They can expand during the tensile process at elevated temperature. Therefore, σ_b decreases to about 150 MPa at 423 K for the three alloys,

Fig. 5 Flow samples of as-cast (a) and die-cast (b) alloys

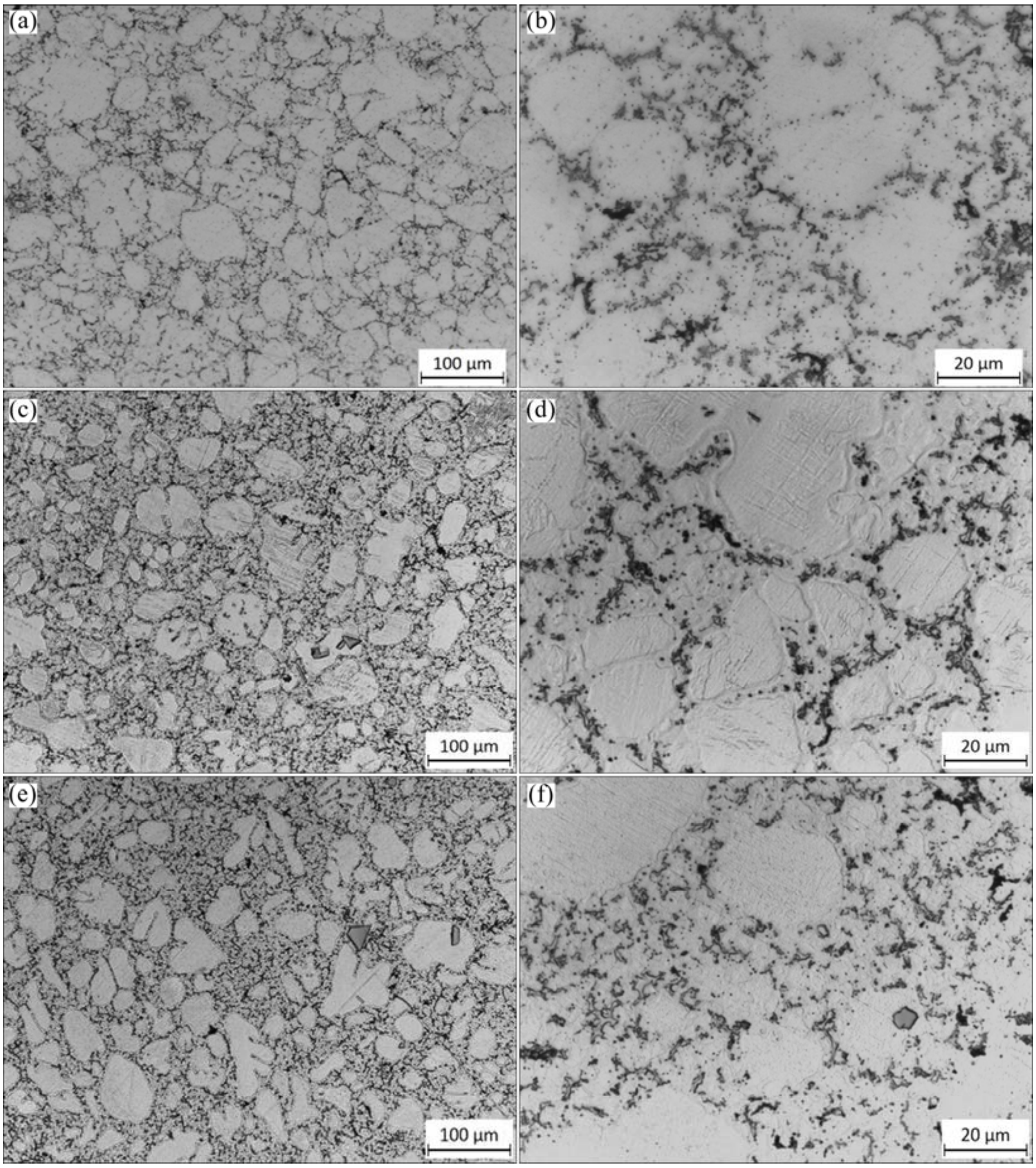

Fig. 6 Optical micrographs of die-cast alloys: (a, b) Mg−6.02Al−1.03Sm; (c, d) Mg−6.05Al−0.98Sm−0.56Bi; (e, f) Mg−5.95Al−1.01Sm−0.57Zn

which is even lower than that of the as-cast. How to reduce the gas cavities for the die-cast sample is a task to be resolved urgently. Researchers often ameliorate the problem by optimizing the die-cast process parameters or using advanced die-cast technology such as vacuum die casting.

Compared with the as-cast state, all die-cast tensile fractures at ambient temperature are different significantly (Figs. 4(b), (d) and (f)). Dimples occupy the majority, and meanwhile become deep. The dimples for Mg−6.05Al−0.98Sm−0.56Bi alloy are shallower than those for the other two alloys, which is consistent with its relatively poor tensile mechanical property.

Under the die-cast condition, the three alloys exhibit more excellent flow property (Fig. 5(b)). The flow lengths reach 1870, 2420 and 2300 mm for Mg−6.02Al−1.03Sm, Mg−6.05Al−0.98Sm−0.56Bi and Mg−5.95Al−1.01Sm−0.57Zn alloys, respectively. Meanwhile, the change in the flow property for die-cast samples is different from that for as-cast samples. It may be related to different flow rules for each element and different microstructures under different cooling conditions.

4 Conclusions

1) The microstructure of as-cast Mg−6.02Al−1.03Sm alloy is composed of α-Mg matrix, discontinuous β-$Mg_{17}Al_{12}$ phase and small block Al_2Sm phase. The rod Mg_3Bi_2 phase precipitates when 0.56%Bi

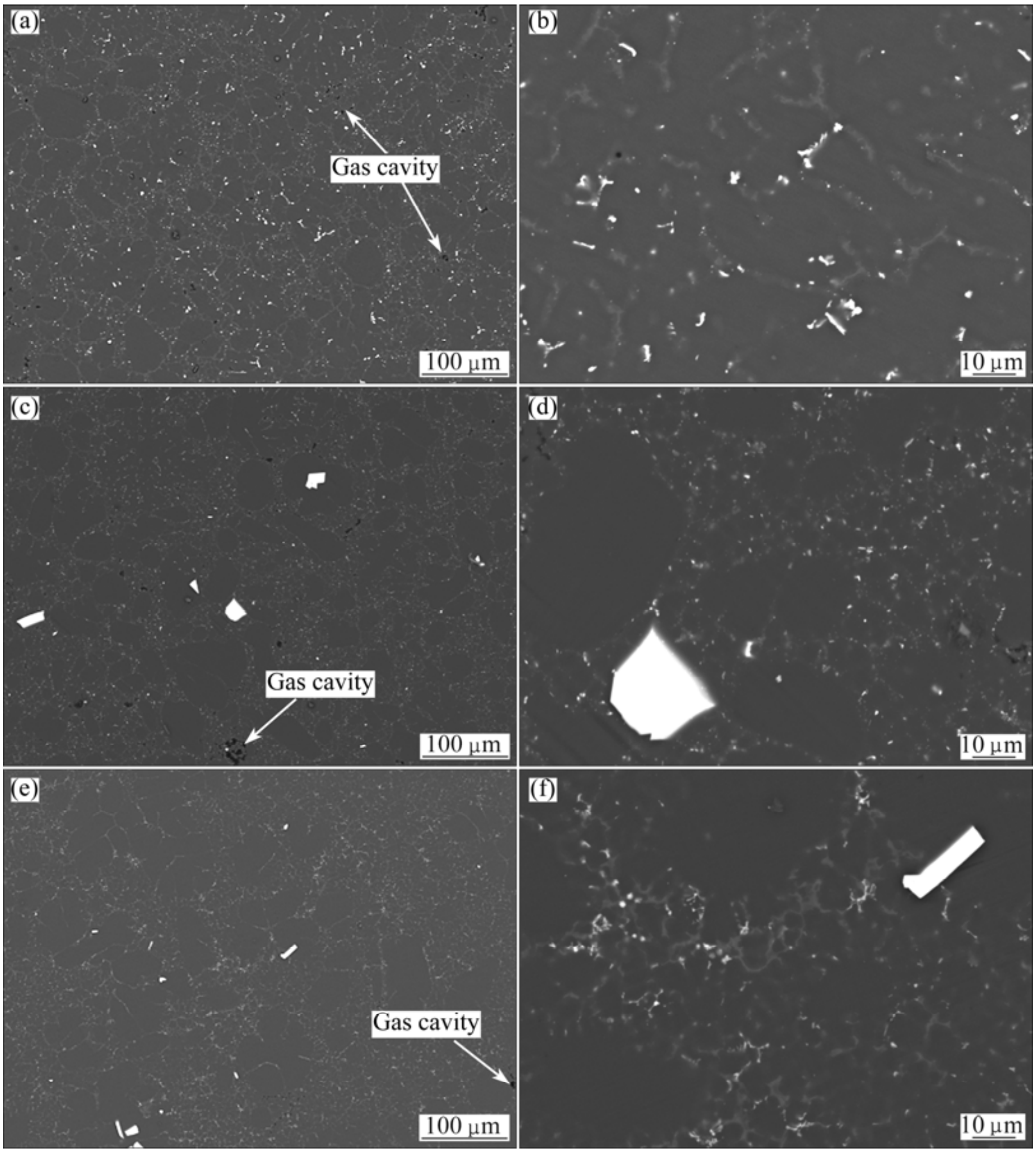

Fig. 7 SEM images of die-cast alloys: (a, b) Mg−6.02Al−1.03Sm; (c, d) Mg−6.05Al−0.98Sm−0.56Bi; (e, f) Mg−5.95Al−1.01Sm−0.57Zn

is added, while the added metal Zn dissolves into α-Mg matrix and β-$Mg_{17}Al_{12}$ phase. The as-cast alloys exhibit excellent tensile mechanical properties. σ_b and δ reach 205−235 MPa and 8.5%−16.0% at ambient temperature, respectively. Meanwhile, they also exceed 160 MPa and 14.0% at 423 K, respectively.

2) The die-cast microstructures are refined obviously, and the broken second phases distribute along the grain boundary dispersedly. The die-cast alloys exhibit better tensile mechanical properties with σ_b and δ of 240−285 MPa and 8.5%−16.5% at ambient temperature, respectively, and excellent flow property with the flow length of 1870−2420 mm.

3) The die-cast tensile fractures at ambient temperature exhibit a typical character of ductile fracture. Deep dimples occupy the majority.

References

[1] POLMEAR I J. Magnesium alloys and applications [J]. Materials Science and Technology, 1994, 10(1): 1−16.

[2] WANG Q D, CHEN W Z, ZENG X Q, LU Y Z, DING W J, ZHU Y P, XU X P. Effects of Ca addition on the microstructure and mechanical properties of AZ91 magnesium alloy [J]. Journal of Materials Science, 2001, 36 (12): 3035−3040.

[3] XU C X, JU H, ZHOU Y. Effect of Ca on microstructure and properties of Mg−Al−Si alloys [J]. Advanced Materials Research, 2011, 194−196: 1369−1373.

[4] LOU Yan, BAI Xing, LI Luo-xing. Effect of Sr addition on microstructure of as-cast Mg−Al−Ca alloy [J]. Transactions of Nonferrous Metals Society of China, 2011, 21(6): 1247−1252.

[5] YUAN G Y, LIU Z L, WANG Q D, DING W J. Microstructure refinement of Mg−Al−Zn−Si alloys [J]. Materials Letters, 2002, 56: 53−58.

[6] LU Y Z, WANG Q D, ZENG X Q, ZHU Y P, DING W J. Behavior of

Mg−6Al−xSi alloys during solution heat treatment at 420 °C [J]. Materials Science and Engineering A, 2001, 301: 255−258.

[7] ASL K M, TARI A, KHOMAMIZADEH F. The effect of different content of Al, RE and Si element on the microstructure, mechanical and creep properties of Mg−Al alloys [J]. Materials Science and Engineering A, 2009, 523(1−2): 1−6.

[8] YOKOBAYASHI H, KISHIDA K, INUI H, YAMASAKI M, KAWAMURA Y. Enrichment of Gd and Al atoms in the quadruple close packed planes and their in-plane long-range ordering in the long period stacking-ordered phase in the Mg−Al−Gd system [J]. Acta Materialia, 2011, 59(19): 7287−7299.

[9] SON H T, LEE J S, KIM D G, YOSHIMI K, MARUYAMA K. Effects of samarium (Sm) additions on the microstructure and mechanical properties of as-cast and hot-extruded Mg−5wt%Al−3wt%Ca-based alloys [J]. Journal of Alloys and Compounds, 2009, 473(1−2): 446−452.

[10] LI Ke-jin, LI Quan-an, JING Xiao-tian, CHEN Jun, ZHANG Xing-yuan. Effects of Sb, Sm and Sn additions on the microstructure and mechanical properties of Mg−6Al−1.2Y−0.9Nd alloy [J]. Rare Metals, 2009, 28(5): 516−522.

[11] ZHANG Shi-chang, WEI Bo-kang, CAI Qi-zhou, WANG Li-shi. Effect of mischmetal and yttrium on microstructures and mechanical properties of Mg−Al alloy [J]. Transactions of Nonferrous Metals Society of China, 2003, 13(1): 83−87.

[12] ZHANG J H, YU P, LIU K, FANG D Q, TANG D X, MENG J. Effect of substituting cerium-rich mischmetal with lanthanum on microstructure and mechanical properties of die-cast Mg−Al−RE alloys [J]. Materials and Design, 2009, 30(7): 2372−2378.

[13] ZHANG J H, LENG Z, LIU S J, ZHANG M L, MENG J, WU R Z. Structure stability and mechanical properties of Mg−Al-based alloy modified with Y-rich and Ce-rich mischmetals [J]. Journal of Alloys and Compounds, 2011, 509(20): L187−L193.

[14] HUANG Zheng-hua, GUO Xue-feng, ZHANG Zhong-ming. Effects of Ce on damping capacity of AZ91D magnesium alloy [J]. Transactions of Nonferrous Metals Society of China, 2004, 14(2): 311−315.

[15] DEAN J A. Lange's handbook of chemistry [M]. 15th ed. New York: McGraw-Hill Press, 1999: 429−435.

Mg−Al−Sm 系耐热镁合金的显微组织和力学性能

黄正华，戚文军，徐 静，蔡 畅

广州有色金属研究院，广州 510650

摘 要：分析铸态和压铸态 Mg−6.02Al−1.03Sm、Mg−6.05Al−0.98Sm−0.56Bi 和 Mg−5.95Al−1.01Sm−0.57Zn 合金的显微组织和相组成，测试其拉伸力学性能与流动性能。结果表明，Mg−6.02Al−1.03Sm 合金铸态组织由α-Mg 基体、半连续的β-$Mg_{17}Al_{12}$ 相和高热稳定性的小块状 Al_2Sm 相组成。添加 Bi 后生成杆状 Mg_3Bi_2 相，而添加的 Zn 固溶于α-Mg 基体和β-$Mg_{17}Al_{12}$ 相中。铸态合金呈现优异的拉伸力学性能，室温时其抗拉强度(σ_b)和伸长率(δ)分别达到 205~235 MPa 和 8.5%~16.0%，而 423 K 时分别超过 160 MPa 和 14.0%。压铸态组织明显细化，第二相发生破碎，且弥散分布。压铸态合金呈现更高的拉伸力学性能和优异的流动性能，室温σ_b和δ分别达到 240~285 MPa 和 8.5%~16.5%，流动长度可达 1870~2420 mm。压铸态室温拉伸断口呈现明显的断裂特征。

关键词：耐热镁合金；Mg−Al−Sm 合金；显微组织；力学性能；流动性能；断口形貌

(Edited by Wei-ping CHEN)